Original Article
Identification and biological characteristics of clear cell renal cell carcinoma associated urine-derived stem cells

Shengjun Luo[1], Lan Shao[2], Ruizhi Geng[3], Qingyuan Liu[1], Wencheng Jiang[1], Mengjia Gong[4], Yuanyuan Zhang[5], Yunfeng He[1]

Departments of [1]Urology, [2]Rehabilitation, The First Affiliated Hospital of Chongqing Medical University, Chongqing, China; [3]Department of Urology, University of Tübingen Hospital, Tübingen, Germany; [4]Pediatric Research Institute, Children's Hospital of Chongqing Medical University, Chongqing, China; [5]Wake Forest Institute of Regenerative Medicine, Wake Forest University, Winston Salem, NC, USA

Abstract: Urine-derived stem cells (USC) are isolated from voided urine and have demonstrated potential for use in tissue engineering and regenerative medicine therapies. Clear cell renal cell carcinoma (ccRCC) is a common urological malignancy that originates in the kidney. Since USC also originate in the kidney, the objective of this study was to investigate any biological differences between USC isolated from healthy patients and those isolated from ccRCC patients (rc-USC). We found that USC can be isolated from the voided urine of ccRCC patients (rc-USC) and have a morphology and function similar to those isolated from healthy donors. However, the rc-USC showed greater proliferation and invasion capacity than USC, and possessed some features of cancer cells; but the rc-UC were not able to form xenografts when implanted *in vivo*. We further performed RNA sequencing of rc-USC and USC and found several differentially expressed lncRNAs and mRNAs; however subsequent GO and KEGG enrichment analysis showed few pathway differences between these cells. Bioinformatic analyses and RT-PCR showed the expression of several known ccRCC-related genes in rc-USC expressed, as compared to USC derived from healthy donors. This study demonstrates that rc-USC displayed several cellular and genetic features of ccRCC cells, which suggests that this population of cells could provide a non-invasive approach for for the diagnosis, predication, disease modeling and therapeutic strategies targeting ccRCC.

Keywords: Urine-derived stem cells, mesenchymal stromal cells, RNA sequencing, tumor-associated stromal cells, clear cell renal cell cancer

Introduction

Urine-derived stem cells (USC) possess progenitor cell characteristics and are easily obtained through noninvasive methods, as they have been successfully isolated and expanded from voided human urine [1, 2]. These cells display many features of pluripotent stem cells (PSC) and have been differentiated into multipotent cells, including cells of the endothelial, osteogenic, chondrogenic, adipogenic, skeletal myogenic, and neurogenic lineages [2-4]. Furthermore, induced USC have been shown to form bone, muscle, fat, endothelial tissue and urothelial tissue following implantation *in vivo* [2]. These characteristics make USC an ideal cell source for tissue engineering and regenerative medicine therapies [1, 2, 5, 6], and are currently being tested for conditions such as erectile dysfunction, urinary incontinence and stricture, and type 2 diabetes [3, 4, 7-10]. Previous studies have suggested that the origin of USC is the kidney and that USC are likely to be transitional cells at the parietal cell or podocyte interface that originate from renal tissue [2, 3, 5, 11].

Renal cell carcinoma (RCC) is a common urological malignancy, accounting for approximately 2% of the total incidence of malignant tumors, while and clear cell RCC (ccRCC) is the most common subtype [12]. ccRCC denotes cancer that originates from the renal tubule epithelium [12], which is near the possible site of origin of USC.

In addition, tumors can be considered "wounds that never heal", and in response to cues from a tumor, stromal cells are continuously recruit-

ed to and become integral components of the tumor microenvironment (TME) [13]. Therefore, there may be a relationship between USC and ccRCC. To our knowledge, no study has explored the relationship between ccRCC and USC. This study was conducted to investigate whether USC could be isolated from the voided urine of patients with ccRCC (rc-USC) and to elucidate the biological and genetic differences between rc-USC and USC.

Materials and methods

Culture of urine-derived cells

The collection of urine was approved by the Ethics Committee of Chongqing Medical University (CQMU). A total of 20 voided urine samples were obtained before surgery from 10 patients (7 males and 3 females, ranging from 45-66 years old) with typical ccRCC imaging manifestations, maximum diameter of neoplasm >4 cm, without distance metastasis and hematuria, at the First Affiliated Hospital of CQMU. Each sample contained at least 150 ml of urine from one urination, and 12 samples from 6 matched healthy adults (4 males and 2 females, ranging from 38-59 years old) were obtained as controls. After collection, cell culture was performed as previously described [1, 11]. Briefly, sterile fresh urine samples were centrifuged at 1,500 rpm for 5 minutes, and the urine supernatant was discarded. The cell pellets were resuspended and plated in 24-well tissue culture plates with USC culture medium composed of keratinocyte-serum free medium (KSFM) and embryonic fibroblast medium (EFM) at a 1:1 ratio [1, 2, 11]. The cells that remained unattached to the plate were washed away when the medium was changed, and only the cells that were attached to the culture plates were used (P0). When the cells reached 60%-70% confluence, they were transferred into 6-well plates (P1). Finally, the USC were transferred to a 150 mm culture dish (P2) for expansion. For most experiments, USC at p2-4 were used. If the surgical pathology results were not from Fuhrman G2 ccRCC, the samples were discarded. Analysis of cell morphology under an inverted microscope and assays of the colony-forming ability of the USC from ccRCC patients (rc-USC) and healthy controls (USC) were carried out during passaging.

Cell proliferation and colony formation assay

Cell viability and clonogenicity were determined by CCK-8 and colony formation assays. Briefly, rc-USC and USC at P2 were seeded and cultured separately in 96-well plates at a density of 1,000 cells per well, and the culture medium was changed every two days. After 0, 1, 3, 5, 7, and 9 days of culture, CCK-8 reagent (Dojindo, Japan) was added to each well (20 μl per well) and incubated for 4 hours at 37°C before measurement. The absorbance was measured at 490 nm by a spectrophotometer (Thermo, USA).

Similarly, the experimental cells (100 cells/well) were cultured in 6-well plates for 10 days. After being washed with cold PBS, the cells were fixed with 4% paraformaldehyde for 10 minutes and stained with crystal violet for 20 minutes at room temperature. The cell clones in individual wells were imaged and counted (only more than 50 cells/cluster were calculated) under a light microscope (Olympus, Japan).

Flow cytometry

Both rc-USC and USC at P2 were trypsinized and stained with the following specific anti-human labeled antibodies: CD31-FITC, CD34-PE, CD73-PE, CD90-FITC, CD105-FITC, and CD146-PE (BD Biosciences, USA). FITC-conjugated IgG and PE-conjugated IgG were used as isotype controls (BD Biosciences, USA) to determine background fluorescence. After staining, the cells were analyzed using a CytoFLEX Flow Cytometer (Xitogen, Suzhou, China). A total of 1×10^7 rc-USC or USC were immobilized separately with 70% ethanol that was prechilled for 8 hours. Ethidium bromide was added for 30 minutes at 4°C, and then the cells were analyzed by flow cytometry to observe the cell cycle. A total of 1×10^5 rc-USC and USC were resuspended separately in PBS, stained with annexin V-FITC and PI for 20 minutes in the dark, and then analyzed by flow cytometry to observe apoptosis. All procedures followed the manufacturer's instructions, and the data were analyzed with FlowJo Software.

Cell migration and invasion assay

Wound healing, Transwell migration and invasion assays were performed. Briefly, rc-USC and USC at P2 were seeded in 6-well plates at

a density of $5×10^5$ cells per well for the wound healing assay. Then, the single confluent cell layer was scraped with a 200-microliter sterile pipette tip to make a scratch through the layer of cells. After washing twice with PBS, medium without FBS was added to the cells. The scratched area was photographed on days 0, 1 and 2. Data were analyzed with Image-pro software.

Cells from each group were seeded into the upper wells of Transwell chambers ($2×10^5$ cells/well) in 200 μl of culture medium without FBS, and 500 μl of medium containing 10% FBS was added to the bottom wells for the cell migration assay. After 24 hours of incubation, the medium was removed from the upper well, and the noninvasive cells were removed with a cotton swab. The bottom wells were fixed and stained as described above and then photographed under a light microscope and measured at 570 nm with a spectrophotometer. The cell invasion assay was performed similarly to the migration assay, except 100 μl/well Matrigel (BD Biosciences, USA) diluted at a ratio of 1:8 was added to the upper wells.

Liquid-based cytology (LBC) assay

Cultured rc-USC and USC from P4 and voided fresh urine from ccRCC patients and normal adults were collected for LBC to observe the morphologic differences between the different cells. Each group contained 2 samples from different individuals. Cultured cells were washed twice with PBS before the following experiment. The samples were centrifuged at 3,000 rpm for 5 minutes, and the supernatant was discarded. The deposited cells were transferred into the liquid fixative and mixed thoroughly for 20 minutes. The mixture was further centrifuged at 3,000 rpm for 5 minutes. After removing the supernatant, Tris buffer solution (2 ml, pH=7.2) was added to the cells. The supernatant was discarded again, and the cells were mixed with Tris buffer solution (2 ml, pH=7.2). A thin layer of cells was deposited naturally onto a positively charged glass slide coated with the mixture, followed by HE staining. Finally, all HE-stained cells were examined under a light microscope (Olympus, Japan).

Urothelial and smooth muscle differentiation assay

A single clone was used for differentiation of cells into two cell lineages, urothelial cells (UCs)

and smooth muscle cells (SMCs), as previously reported [11], to determine whether rc-USC had the same capacity for multipotential differentiation as USC. Briefly, rc-USC and USC at P2 were plated and induced to differentiate into UCs and SMCs by culture in specific induction medium for 14 days at a density of 1500 cells/cm^2. For urothelial differentiation, equal volumes of KSFM and EFM containing 40 ng/ml epidermal growth factor (EGF) were used [11]. For SMC differentiation, DMEM with 10% FBS containing 2.5 ng/ml transforming growth factor β1 (TGF-β1) and 5 ng/ml platelet-derived growth factor (PDGF) was used [11]. Both differentiation media were replaced every three days. All growth factors were purchased from R&D Systems (Minneapolis, MN). Cell morphology was observed by inverted microscopy (Olympus, Japan).

The rc-USC and USC clones were cultured on 8-well chambered slides (Thermo Scientific, UK) for staining with UC markers (AE-1) and SMC markers (α-SMA) after 14 days of differentiation. The slides were fixed with 4% paraformaldehyde for 20 minutes at room temperature, extracted with 0.3% Triton X and washed several times with PBS. Lineage-specific primary antibodies (Abcam, UK) were diluted (AE-1, 1:200; α-SMA, 1:100) and incubated with the cells overnight at 4°C. After rewarming for 1 hour at room temperature, the cells were washed with PBS three times to remove the primary antibody. A secondary antibody conjugated to fluorescein-isothiocyanate (FITC) was used to visualize the primary antibody (green), and the cells were incubated at room temperature for 1 hour in the dark. Nuclei were stained with DAPI (blue). Images were captured with a fluorescence microscope (Olympus, Japan).

Fluorescence in situ hybridization (FISH) assay

Commercially available FISH centromere-specific probes (CSPs) were used for each critical chromosome (3p11.1-q11.1, 7p11-q11, 17p11.1-q11.1 and Y) to detect chromosomal alterations in rc-USCs, USC and tumor tissues [14-16]. Briefly, slides of cultured rc-USC (2 males and 1 female) and USC (2 males and 1 female) from P4 were produced similarly to the slides used for LBC, except that a different fixative (3:1 methanol: acetic acid) was used, the cells were treated with protease, and the cells were not stained. Formol-fixed and paraffin-

embedded cancer tissue sections (5 μm) from the same patients from whom the tested rc-USC were isolated were deparaffinized with toluene and dehydrated using an ethanol series (100%, 90%, and 70%, for 3 minutes each); 10 μl of FISH probe (Anbiping, Guangzhou, China) was applied to the slide, and the tissue was denatured for 4 minutes at 85°C and incubated overnight. The slides were washed according to the manufacturers' instructions, and the nuclei were counterstained with DAPI (Leagene, Beijing, China). Cells were viewed with a fluorescence microscope (Olympus, Japan) and analyzed with FISH 3.0 software. The probe signals were visualized as follows: a green single-bandpass filter was used for chromosomes 3, 7 and 17, and a red single-bandpass filter was used for chromosome Y. The FISH patterns were determined by analyzing 100 nonoverlapping nuclei to detect trisomy of chromosomes and the loss of chromosome Y.

Karyotype analysis

Karyotype analysis was performed to test the chromosomal stability of cells from various passages as previously described [1, 5]. One sample of rc-USC and 1 sample of USC from P2 and P7 were used, and the analysis was repeated in triplicate. Briefly, cultured cells were treated with colcemid (0.02 μg/mL) and hypotonic solution (0.075 M KCl) and then fixed with methanol-to-acetic acid fixative at 4°C. The metaphase spreads were applied to slides and digested with trypsin, followed by staining with Giemsa to generate G bands. Cytogenetic analysis was performed under microscopy (Zeiss, Jena, Germany), and Metasystems IKaros software was used to analyze and capture the chromosome images.

Quantitative real-time PCR (RT-PCR)

Total RNA was extracted from 3 individual groups of cells from P3 according to the TRIzol method. After quantification by spectrophotometry, the RNA samples were reverse-transcribed into cDNA using the Prime Script RT reagent kit (TaKaRa, Japan) according to the manufacturer's protocols. The expression levels of the mRNAs and lncRNAs of the tumor-associated genes were determined to confirm the differences between the two types of cultured cells, and GAPDH was used as an endogenous control [17-20]. The 20 μl amplification reaction consisted of 0.8 μl each of the sense and antisense primers (Table S1), 2.0 μl of the cDNA template, and 10 μl of the DNA polymerase SYBR Premix Ex TaqTM II. After the mixture was vortexed and shaken, a fluorescent polymerase chain reaction detection system (Bio-Rad, USA) was used. The data were analyzed by the $2^{-\Delta\Delta Ct}$ method.

Immunohistochemistry

Immunohistochemical staining of formalin-fixed, paraffin-embedded sections of cancer tissues and paracarcinoma tissues cultured from rc-USC from the urine of 3 ccRCC patients was performed. Briefly, after deparaffinization in xylene and rehydration in a series of ethanol solutions, the tissue sections were boiled with sodium citrate buffer in a steamer for antigen retrieval and treated with 3% hydrogen peroxide solution to block potential endogenous peroxidase activity. Next, the sections were incubated with 10% normal horse serum in Tris-buffered saline (TBS) for 30 minutes at room temperature and then with anti-PAX2 antibody (1:500, Epitomics), anti-ALDH1 antibody (1:200, Epitomics), anti-NCAM1 (1:100, Abcam), and anti-SIX2 (1:50, Santa Cruz Biotechnology) for 1 hour at room temperature separately. After 3 washes with PBS (3 minutes per wash), the sections were further incubated with the corresponding secondary antibodies for 20 minutes at 37°C. After another 3 PBS washes, the slides were treated with 3,3'-diaminobenzidine (Zhongshan Golden Bridge Biotechnology) and examined under a microscope (Olympus, Japan). The histochemical scores (H-scores) were used for quantification analysis by two pathologists based on the staining intensity and percentage of positive cells, as described previously [21].

RNA sequencing

Another four samples of rc-USC of G2 ccRCC (group A) and 4 samples of USC (group B) at P2 were prepared for RNA sequencing (including lncRNA and mRNA) and sequenced by Genechem (Shanghai, China). The sequencing method and data analysis were described in the Supplementary Methods.

Bioinformatics analysis

Bioinformatics analysis was used to explore the origin of the changes in rc-USC. We searched

for 'renal clear cell carcinoma' in the TCGA database, and data containing carcinoma and paracarcinoma specimens from the same patients were included in further analysis. The trimmed mean M-values were used to standardize the data. The biological coefficient of variation was used for quality control. A negative binomial general linear model was used to calculate the P value. The $\log_2$ (Cancer/Normal) value was also calculated, and the filtering criteria were greater than or equal to 1 and less than or equal to -1.

Tumorigenicity assay

All animal studies were approved by the Ethics Committee of CQMU. Male BALB/c nude mice (4 weeks old) were housed in a pathogen-free facility in the experimental animal center of CQMU. Cultured rc-USC and USC (1×10^7 cells from different individuals) from P4 were injected into 2 sites subcutaneously. Matrigel with normal saline and 786-0 cells (1×10^7) were used as controls. The groups were divided as follows: each group had 4 mice with a one-month follow-up. At the end of the experiment, the mice were sacrificed, and their tumors were dissected and imaged.

Group 1: 0.5 ml of Matrigel® with normal saline as a control.

Group 2: 0.5 ml of Matrigel® with cultured USCs.

Group 3: 0.5 ml of Matrigel® with cultured rc-USCs.

Group 4: 0.5 ml of Matrigel® with 786-0 cells.

Statistical analysis

Data are expressed as the mean ± SD, and SPSS 22.0 and GraphPad Prism 8 software were used for statistical analysis. Differences among groups of flow cytometry, wound healing, PCR and immunohistochemistry score were analyzed by one-way ANOVA, the Student's t-test was used to compare apoptosis and migration and invasion assay. Differences in the cell growth curves were analyzed by repetitive variance analysis. RNA sequencing analyses were presented in supplementary method. P<0.05 was considered statistically significant.

Results

rc-USC can be isolated from the voided urine of ccRCC patients and have a morphology and function similar to those of normal USC

Urine samples were collected from 6 healthy donors and 7 samples were obtained from grade 2 ccRCC patients. Cells were successfully isolated from all of the healthy donors and 6 out of 7 of the ccRCC patients. Single cells were detected in centrifuged urine from both populations and both displayed a similar morphology after HE staining (**Figure 1A**). Flow cytometry was used to quantify the expression of surface stem cell markers. Both cell populations were strongly positive for embryonic and mesenchymal stem cell markers (CD73, CD90 and CD146) and negative for hematopoietic lineage and immunogenic markers (CD31, CD34 and 105) and only differed in the expression of CD90, which was higher in the rc-USC population (**Figure 1B**). Immunofluorescence staining of the urothelial (AE1) and the myogenic (α-SMA) markers was performed in order to determine the differentiation potential of the cells (**Figure 1C**). After uroepithelial differentiation, both cell populations displayed a cobblestone-like morphology and after induction with myogenic differentiation medium, both cell populations displayed a spindle-like morphology. These results indicate that rc-USC can be isolated from ccRCC patients and possess a similar cell morphology, express similar stem cell markers and demonstrate multipotential differentiation capabilities similar to those of USC from healthy individuals.

rc-USC have a higher rate of proliferation and invasion ability than USC

Single cell clones were observed in rc-USC culture at 3~5 days, and in USC culture at 6-8 days after isolation. The number of established rc-USC colonies was greater than that from the same volume of urine (F=11.67, P=0.01) (Table S2). Additionally, rc-USC showed an increased proliferation rate as compared to USC (**Figure 2A**, **2B**). This was confirmed by cell cycle analysis which showed that the number of rc-USC was lower in G1 and higher in S phase compared to USC (**Figure 2C**). Similarly, the number of cells undergoing apoptosis was significantly lower in rc-USC than USC (**Figure 2D**).
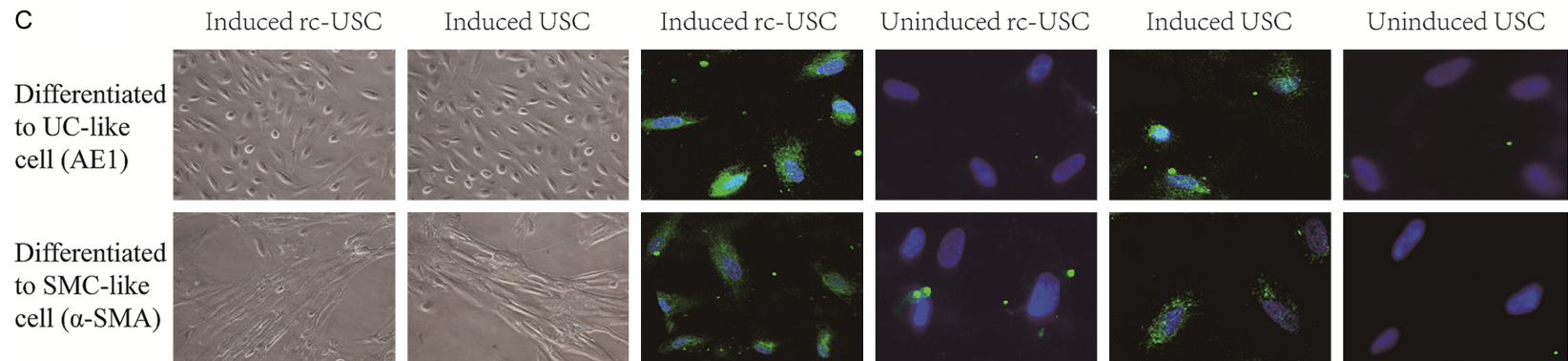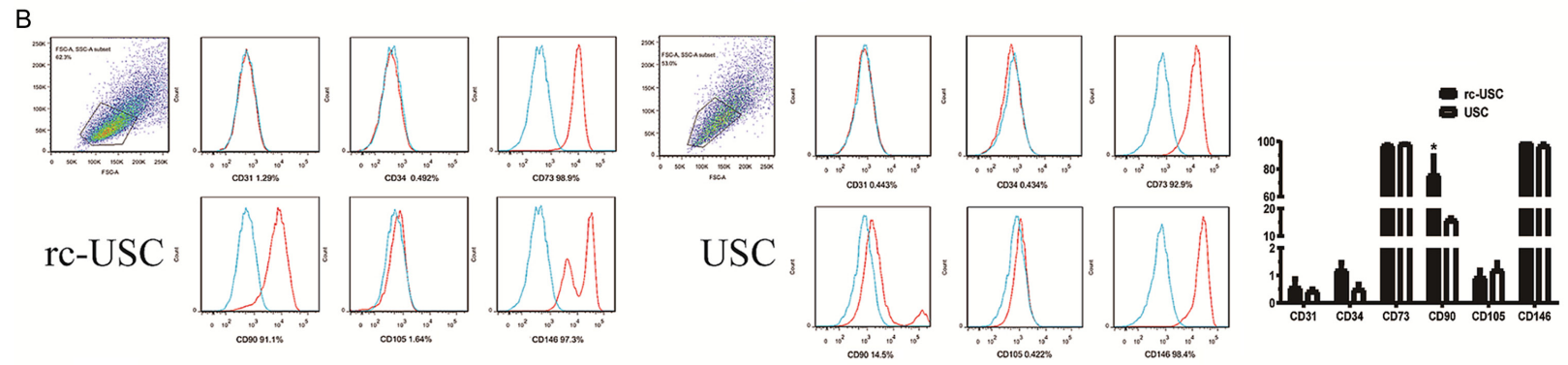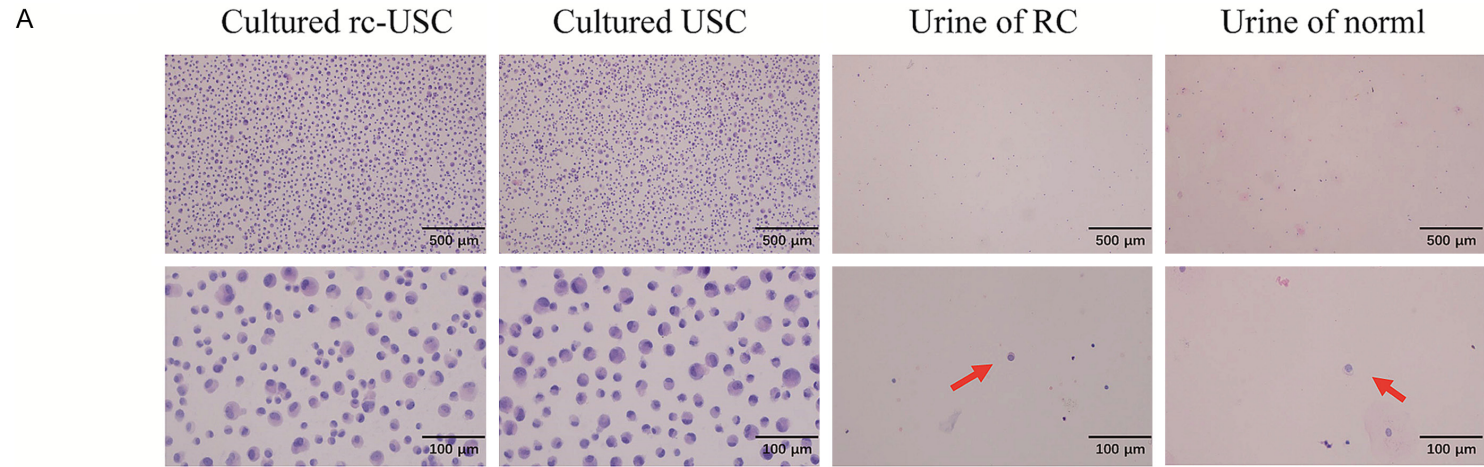
Figure 1. rc-USC have a morphology and function similar to those of normal USC. A. Liquid-based cytology showed that rc-USC and USC were present in centrifuged urine (red arrow) and displayed similar morphologies (scale bar: 500 and 100 microns). B. Flow cytometry was used to assess the expression of stem markers. rc-USC were strongly positive for embryonic/mesenchymal stem cell markers (CD73, CD90 and CD146) and negative for hematopoietic lineage and immunogenic markers (CD31, CD34 and 105), which was similar to the staining observed for USC except for the expression of CD90. C. rc-USC and USC were able to differentiate into urothelial and smooth muscle cells as demonstrated by immunofluorescence staining for the urothelial marker AE1 and the myogenic marker α-SMA. *P<0.05.

Additionally, rc-USC demonstrated a greater migration and invasion capacity as compared to USC (**Figure 2E-G**). These data indicate that rc-USC had a higher proliferation rate and a greater migration and invasion capacity than USC.

rc-USC showed some malignant characteristics but did not form xenografts

Karyotype analysis showed that several chromosomes were deficient in USC, while rc-USC showed the same features at P2 and P7 (**Figure 3A**). The morphology of both rc-USC and USC were similar as observed under an inverted microscope at P0 and P2, but at higher passages (P7) the USC demonstrated large flat cells indicative of senescence that were not detected in the rc-USC (**Figure 3B**). RT-PCR results showed that rc-USC expressed significantly higher levels of genes correlated with tumorigenicity and metastasis (PAX-2, ALDH1, and NCAM1) than USC, but did not differ in the expression of the pluripotent marker SIX-2 (**Figure 3C**). Similar results were found based on the immunohistochemical staining of these proteins in ccRCC tissue and paracarcinoma tissue. ALDH1 and NCAM1 were overexpressed in cancer tissues compared with paracarcinoma tissues (**Figure 3D**, **3E**). ccRCC had several chromosomal aberrations according to the FISH test [14-16]; one of the male experimental cancer samples presented numerous cells with triploid chromosome 3 and chromosome 17. Triploid cells were also found in rc-USC from this patient, but the percentage of triploid cells in rc-USC was a little lower than that in cancer tissue. Cancer sample of the female only presented with triploid chromosome 3, and similar triploid was found in rc-USC. While cancer sample of the other male was almost normal, and the rc-USC from the same patient were also normal; 3 samples of healthy USC were normal (**Figure 3F**). A xenograft model was constructed to verify the tumorigenicity of rc-USC and USC, and normal saline and renal cancer cells (786-0 cells) were used as controls. After one month, transplanted tumors were obtained in only the 786-0 cell group, and H&E staining of xenografts showed clear cell renal cancer cells (**Figure 3G**). These data demonstrated that rc-USC had greater chromosomal and morphological stability than USC after serial passaging. Additionally, rc-USC expressed several proteins associated with ccRCC and presented chromosomal changes similar to those found in cancer tissue based on the FISH assay, but the tumorigenicity of rc-USC was not demonstrated.

Differentially expressed lncRNAs and mRNAs in rc-USC and USC

4 samples of rc-USC from individual patients with RCC and 4 matched samples of USC from healthy donors were used for RNA sequencing and analysis. 1 sample was excluded for the final pathology result was XP11.2/TFE3 RCC, the rest samples were all Grade 2 ccRCC (1 male and 2 females, 2 at T1BN0M0 and 1 at T2N0M0). The basic characteristics of the patients are shown in <u>Table S3</u> and <u>Figure S1</u>. The quality controls were shown in <u>Figure S2</u>. The results showed that there were 76 differentially expressed lncRNAs and 71 differentially expressed mRNAs in rc-USC and USC, respectively (**Figure 4A**, **4B**). Volcano plot analysis showed 41 upregulated and 35 downregulated lncRNAs and 41 upregulated and 30 downregulated mRNAs in rc-USC and USC (**Figure 4C**, **4D**). We listed the top 5 upregulated and top 5 downregulated lncRNAs and mRNAs (<u>Tables S4</u>, <u>S5</u>) with FPKM values >1 and fold change >2 [22, 23]. And chose these lncRNAs for PCR verification of their expression in rc-USC and USC. PCR showed similar upregulated and downregulated trends to sequencing data (**Figure 4E**, **4F**; <u>Table S1</u>). These data indicate there are several differentially expressed genes between rc-USC and USC.
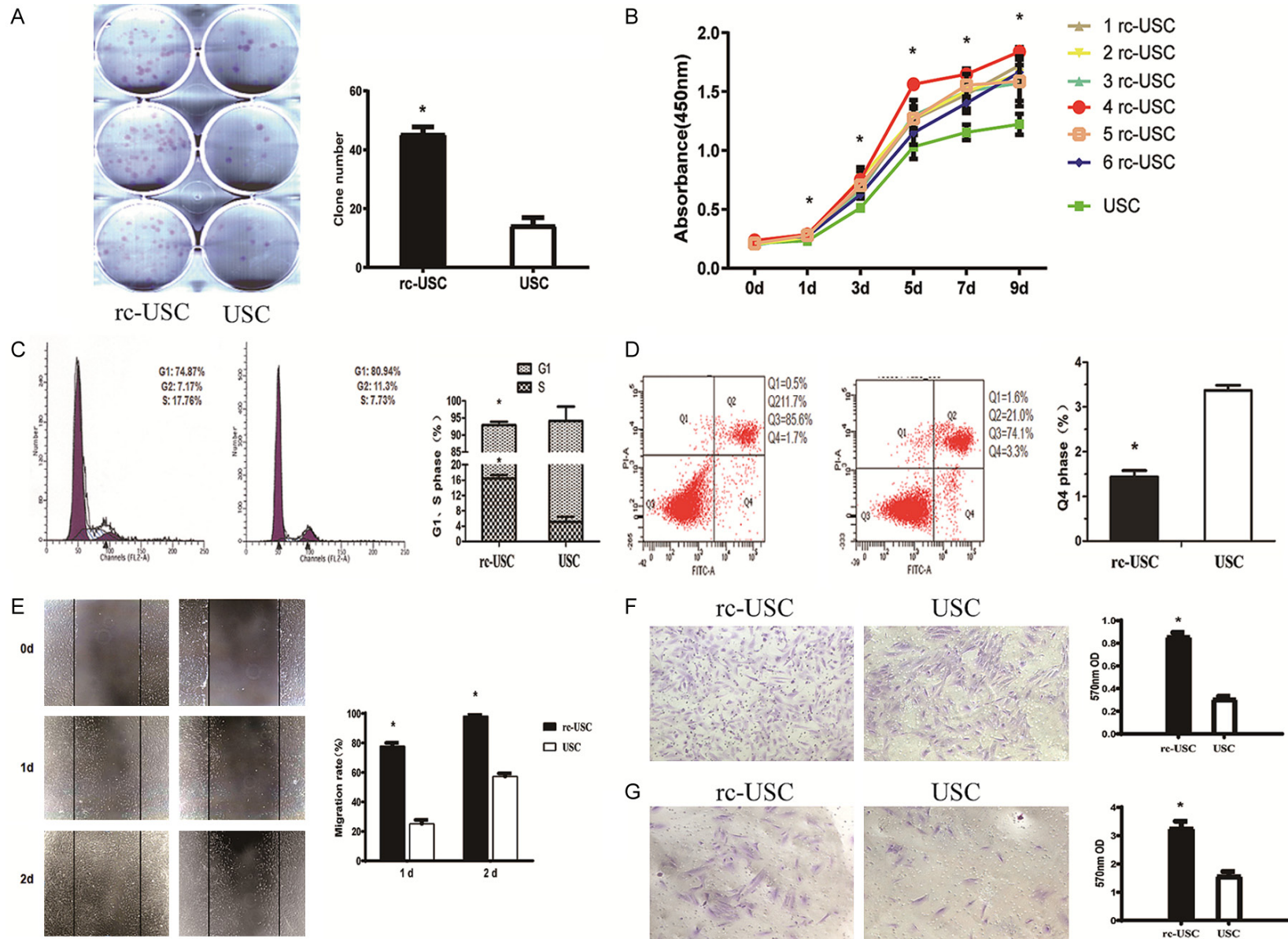
Figure 2. rc-USC showed a faster proliferation rate and increased invasion ability as compared to USC. A. From the same volume of urine, more colonies were formed from rc-USC than USC. B. rc-USC had a faster rate of proliferation as compared to USC. C. The percentage of rc-USC in S phase was significantly higher and the percentage of rc-USC in G1 phase was significantly lower than those of USC. D. rc-USC had lower apoptosis rate than USC. E. rc-USC had stronger wound healing ability than USC. F. rc-USC had stronger migration ability than USC. G. rc-USC had stronger invasion ability than USC. *P<0.05.
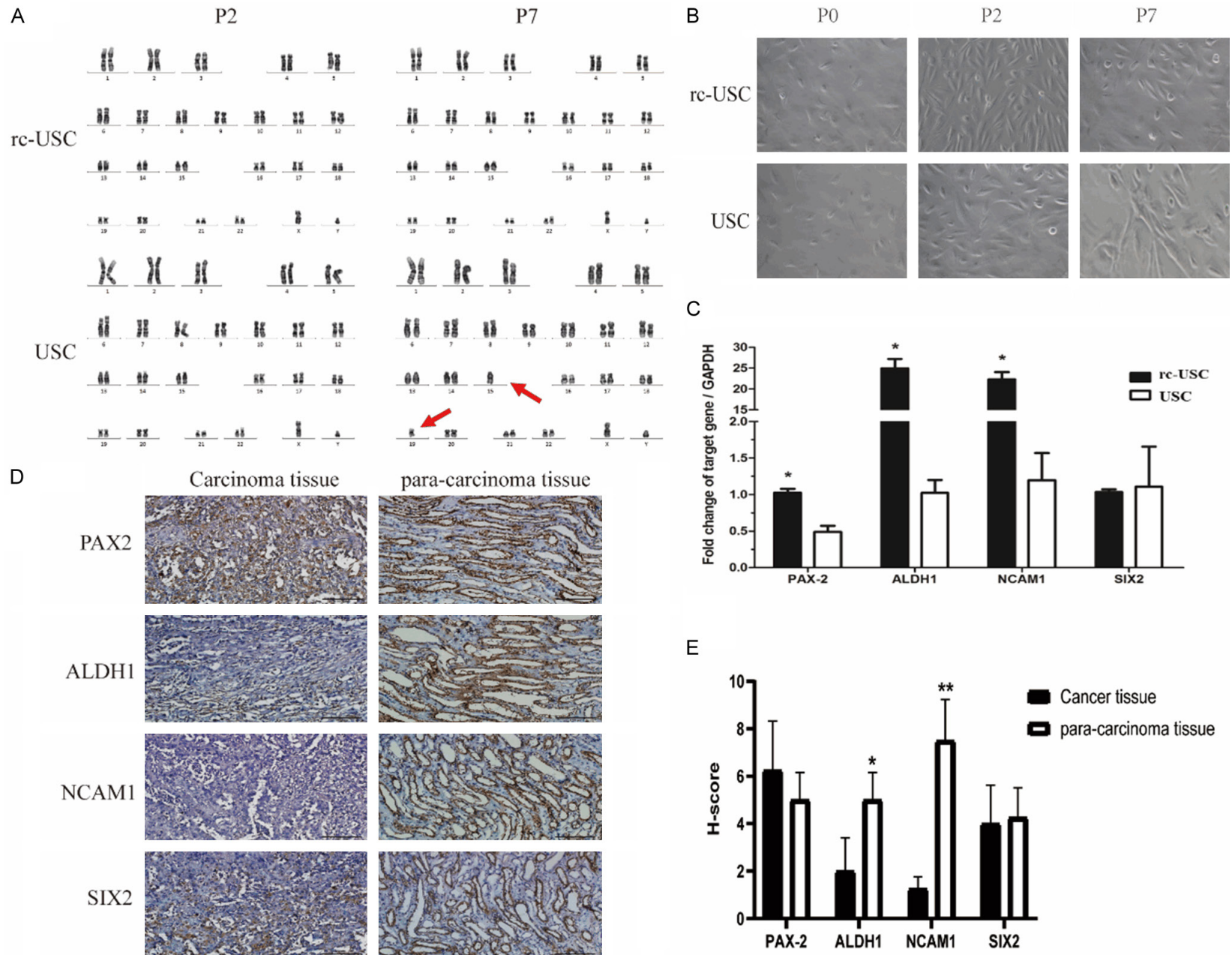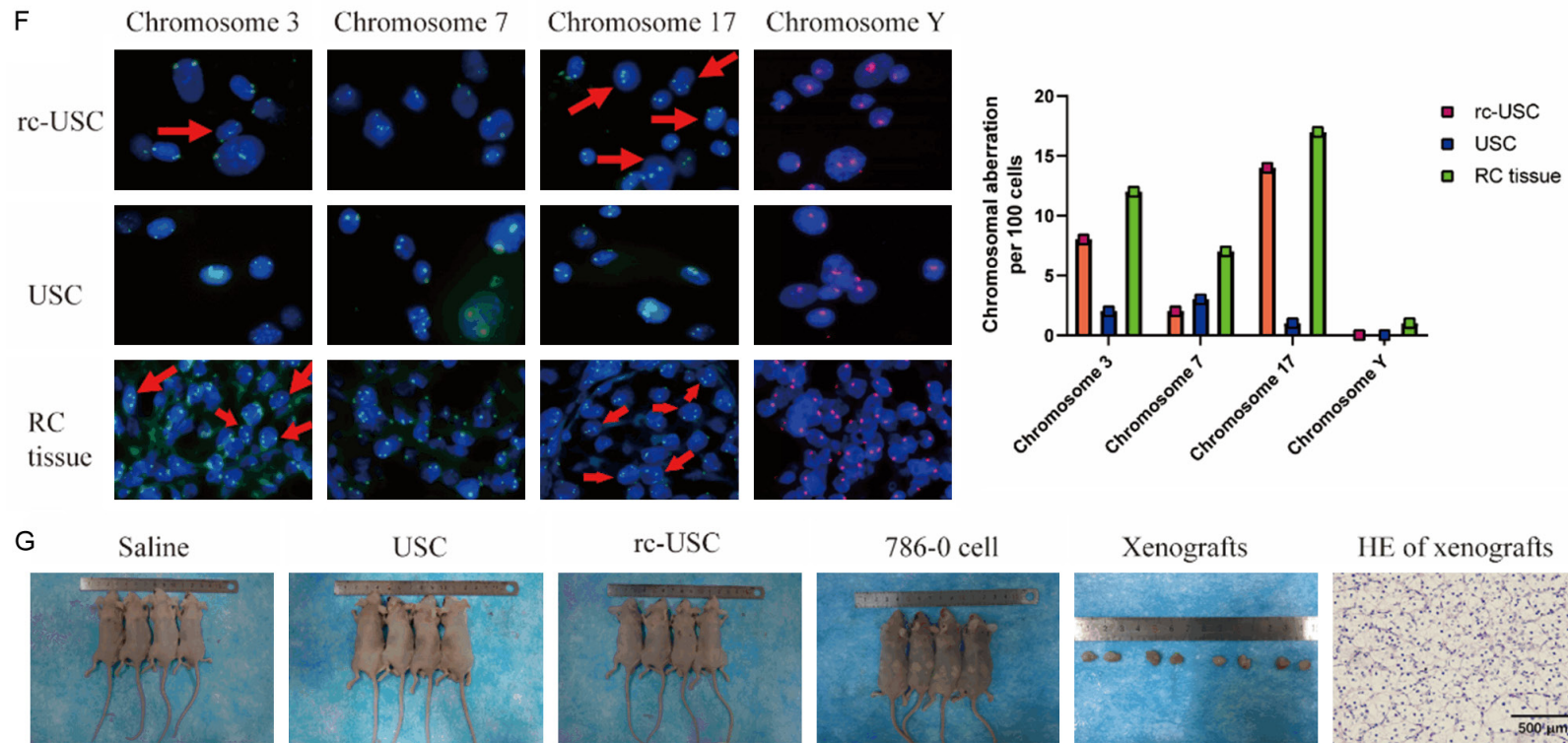
Figure 3. rc-USC express some features of cancer but do not form xenografts. A. Representative chromosome images of rc-USC and USC at passage 2 and passage 7 are shown. Two chromosome deficiencies were found in USC (red arrow), while rc-USC were unchanged at passage 7. B. rc-USC and USC both displayed "rice grain"-like cells, and the morphology of rc-USC was almost unchanged, while that of USC was substantially changed at passage 7. C. rc-USC expressed significantly higher levels of PAX-2, ALDH1, and NCAM1 than USC. D. Immunohistochemical staining showed that the expression of ALDH1 and NCAM1 in cancer tissues was significantly higher than that in paracarcinoma tissues. E. Expression was evaluated quantitatively according to immunohistochemical staining. F. Representative FISH images of ccRCC tissue, rc-USC (from the same patient) and USC are shown; triploid cells are indicated by red arrows, and the number of triploid cells in 100 cells of these paired samples is shown. G. The rc-USC group and USC group did not form tumors after transplantation, and only the 786-0 cell group formed tumors after transplantation; HE staining of xenografts demonstrated the presence of clear cell renal cancer. *P<0.05, **P<0.01.
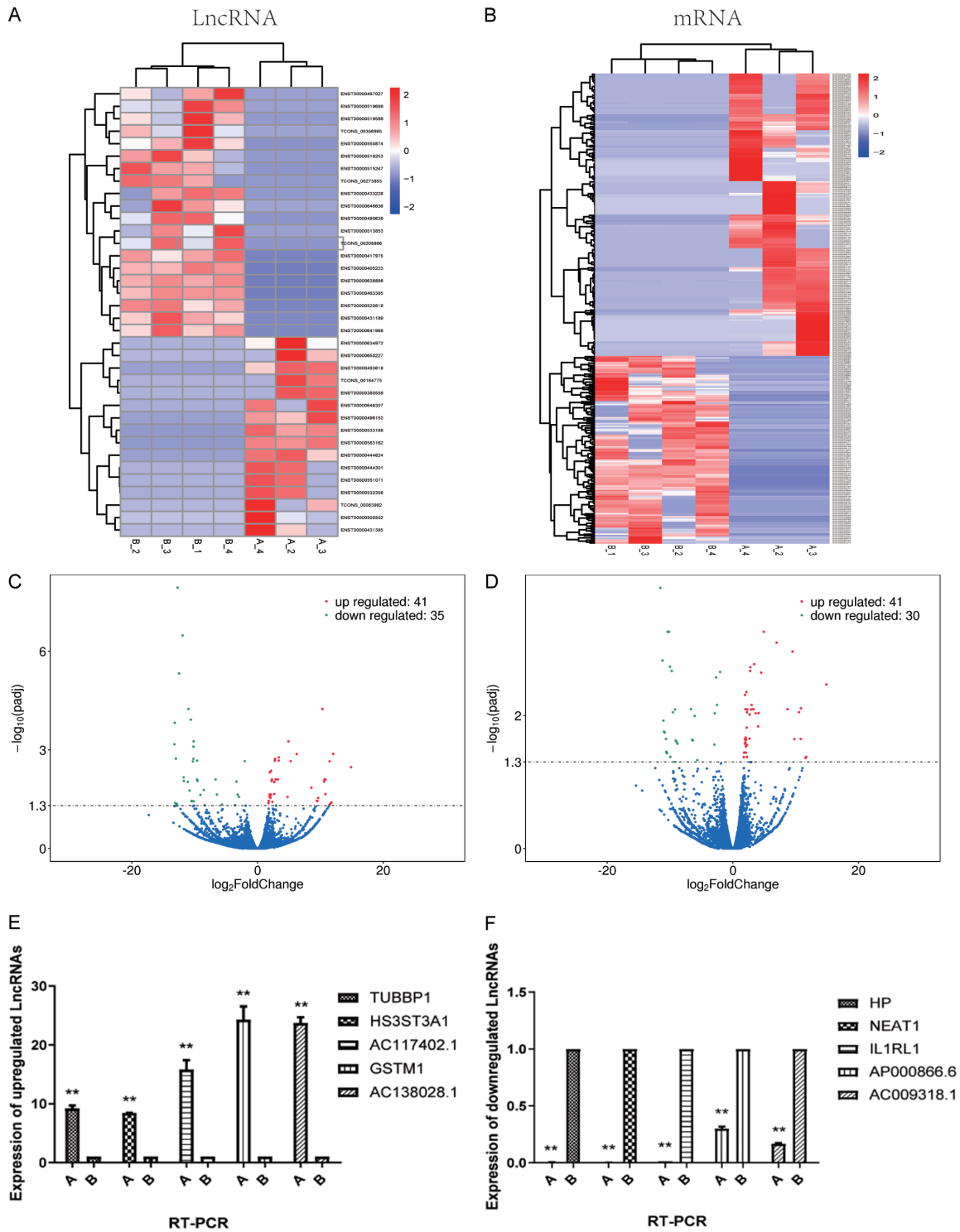
Figure 4. Differentially expressed lncRNAs and mRNAs in rc-USC and USC. (A) Heat map showing the differentially expressed lncRNAs (A) and mRNAs (B) in rc-USC and USC (fold change ≥ 2 and q value ≤ 0.05). (C) Volcano plot of the differentially expressed lncRNAs. Among these lncRNAs, 41 were upregulated and 35 were downregulated in rc-USC and USC. (D) Volcano plot of differentially expressed mRNAs. Among these mRNAs, 41 were upregulated and 30 were downregulated in rc-USC and USC. (E) PCR of upregulated lncRNAs showed similar trends to sequencing data. (F) PCR of downregulated lncRNAs showed similar trends to sequencing data. *P<0.05, **P<0.01.

GO and KEGG enrichment analysis of differentially expressed genes (DEGs)

We performed Gene Ontology (GO) and Kyoto Encyclopedia of Genes and Genomes (KEGG) enrichment analyses of DEGs to explore their potential biological functions in rc-USC. GO enrichment analysis showed no significant differences in the pathways involving the differentially expressed lncRNAs between rc-USC and USC (**Figure 5A**, **5B**), while pathways involved in sarcolemma, proteinaceous extracellular matrix and extracellular matrix showed significant differences according to the differentially expressed mRNAs between rc-USC and USC (**Figure 5C**; Table S6), and. No significant differences in pathways were found in the KEGG enrichment analysis after filtration according to $P_{adj}<0.05$ (**Figure 5A-C**). These data showed that there were few pathway differences between rc-USC and USC; therefore, these results also suggested that rc-USC and USC are the same type of cells.

Bioinformatics analysis

There were 72 paired ccRCC data points (including carcinoma and paracarcinoma tissues) in the TCGA database, and 28 G2 pathological pattern data points were used. Quality control showed that normal (paracarcinoma, N) and cancer (C) samples were separated, which indicated that the data obtained at different times showed high stability and could be used for further analysis (**Figure 6A**). The DEGs of carcinoma and paracarcinoma tissues were shown in **Figure 6B** (Fold change >1). The Venn diagram of the DEGs in carcinoma versus paracarcinoma and rc-USC versus USC was generated without filtration according to $P_{adj}<0.05$ (only P<0.05). The results showed 150 upregulated (**Figure 6C**) and 173 downregulated (**Figure 6D**) overlapping genes. In addition, a Pubmed search was performed to explore the correlations of those DEGs (including differentially pathways related genes) and ccRCC. We found 4 genes were closely associated with ccRCC, and further PCR verified these genes were overexpressed in rc-USC (**Figure 6E**; Table S1). These data suggested that rc-USC might express several ccRCC genes, and these genes may be different due to different types of RCC. Therefore, the genes expressed in rc-USC may be candidate predictive biomarkers to distinguish different types of RCC.

Taken together, these results demonstrate that rc-USC show some cancer features, express cancer-related genes and possess functions similar to that of USC; therefore, rc-USC represented USC that are affected by cancer cells.

Discussion

Zhang first reported that normal stem cells could be isolated and cultured from human urine in 2008 [1], Additional studies confirmed this result and further demonstrated that these cells expressed pluripotent cell markers and differentiation capability as well as other biological functions similar to those of mesenchymal stem cells (MSC) [6, 9, 10, 24, 25]. USC are a safe, noninvasive, efficient and low-cost resource with potential for use in tissue engineering and regenerative therapy [1, 9, 11, 24, 25]. Cells isolated from the urine from the upper urinary tract possess stem cell characteristics similar to those of cells isolated from voided urine [5, 11], suggesting that USC originate from the upper urinary tract. In addition, USC from women who had received kidney transplants from male donors contained the Y chromosome and expressed normal renal cell markers, which demonstrates that USC most likely originate from the kidney [3, 26, 27]. The definite site of origin of USC is still unknown, and previous studies have implied that transitional cells at the parietal cell or podocyte interface that originate from renal tissue are the most likely source [2, 3, 5, 11]. ccRCC is the most common histological type of renal cancer [12]. The origin of renal cancer is in the kidney tubules, which are adjacent to the possible origin sites of USC. These reports prompted us to investigate the potential relationships between USC and ccRCC, and this is the first study to isolate USC from patients with ccRCC, to the best of our knowledge.

In the present study, we isolated a type of progenitor cell from voided urine from patients with ccRCC. Compared with USC, these cells possessed a similar cell morphology and H&E staining pattern under microscopy. In addition, rc-USC expressed stem cell markers similar to those expressed by MSC, including CD73, CD90 and CD146, and were negative for CD31 and CD34 compared with USC [1, 5, 13, 28]. rc-USC had the same ability to differentiate into UCs and SMCs as USC. However, rc-USC had stronger proliferation and invasion ability.

A

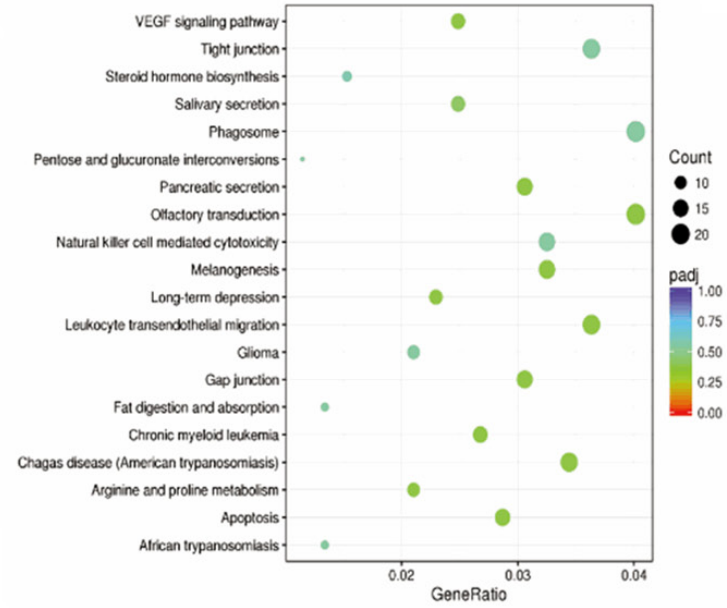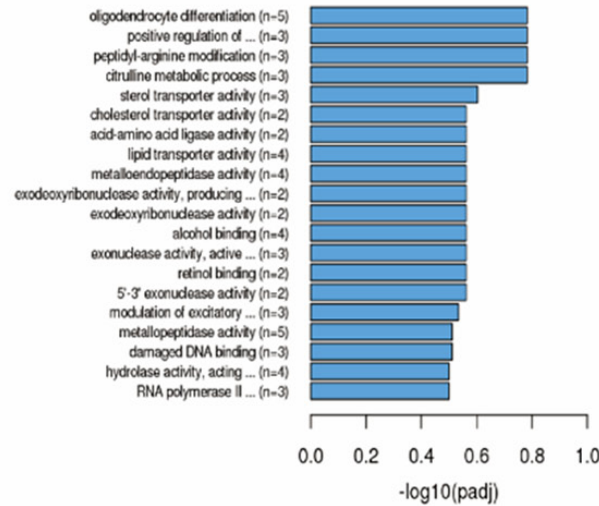GO enrichment analysis   KEGG enrichment analysis
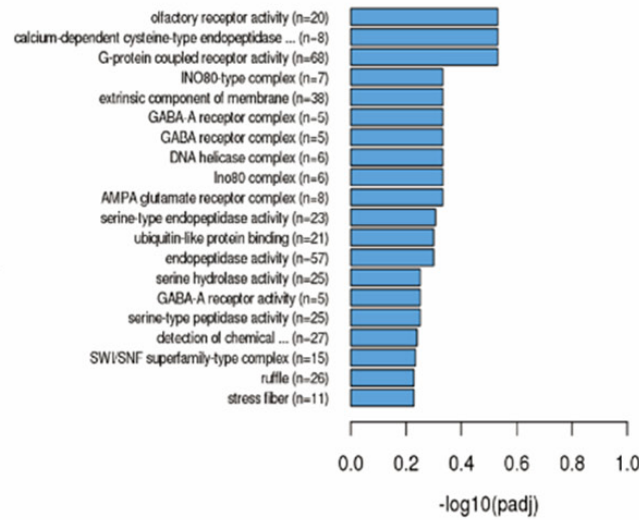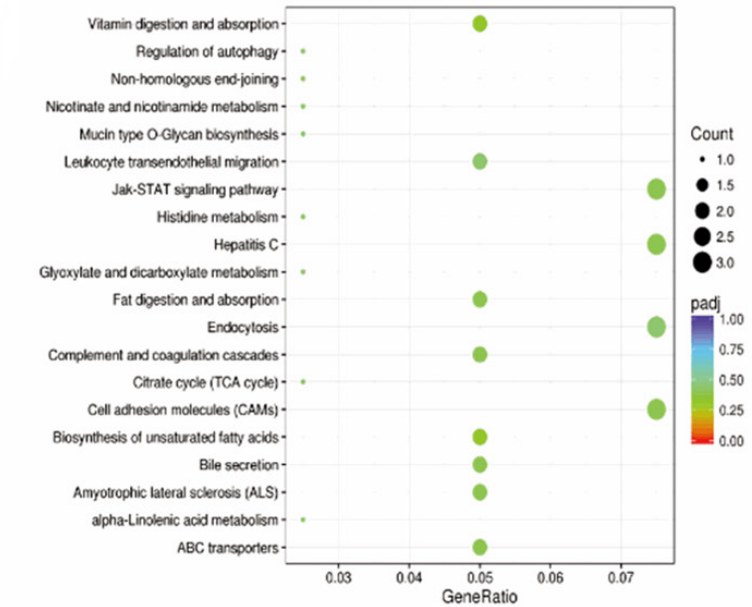
LncRNA co-expression

B

LncRNA co-location
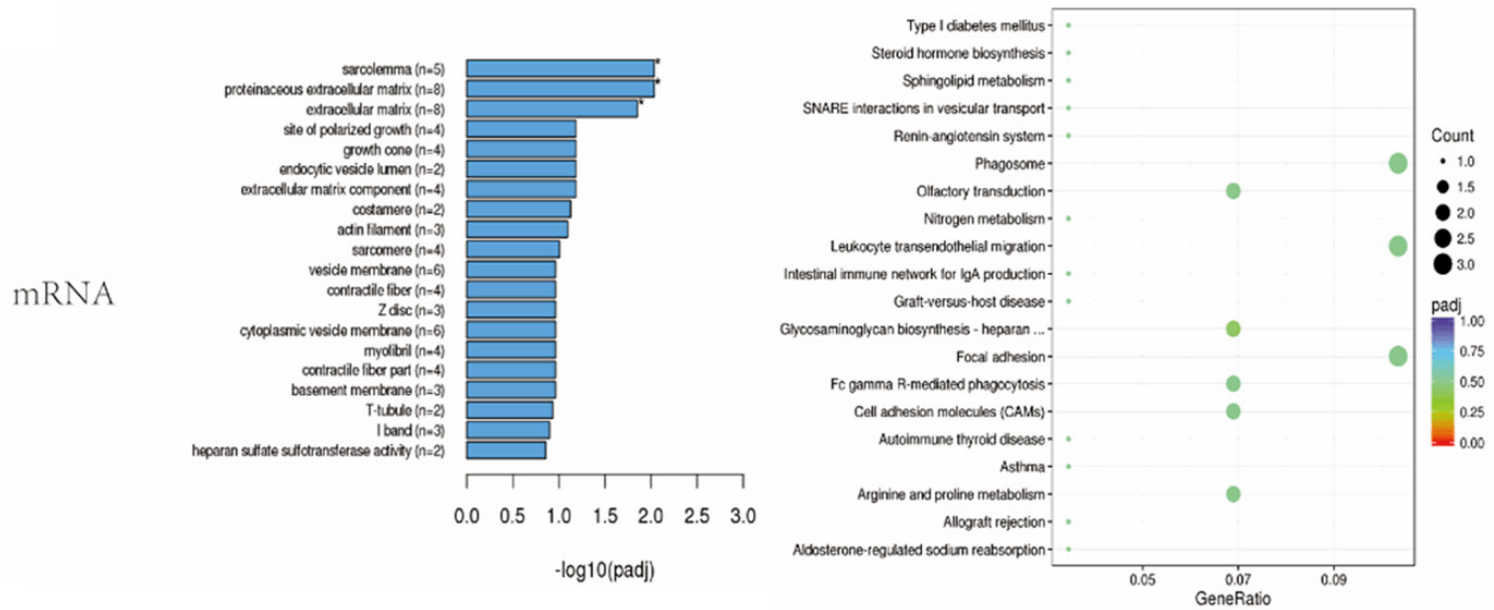
Figure 5. GO and KEGG enrichment analyses of DEGs. A. GO and KEGG enrichment analyses of differentially expressed lncRNAs with coexpression showed no significant differences between rc-USC and USC. B. GO and KEGG enrichment analyses of differentially expressed lncRNAs with colocalization showed no significant differences between rc-USC and USC. C. GO and KEGG enrichment analyses of differentially expressed mRNAs revealed 3 different pathways. *P<0.05.
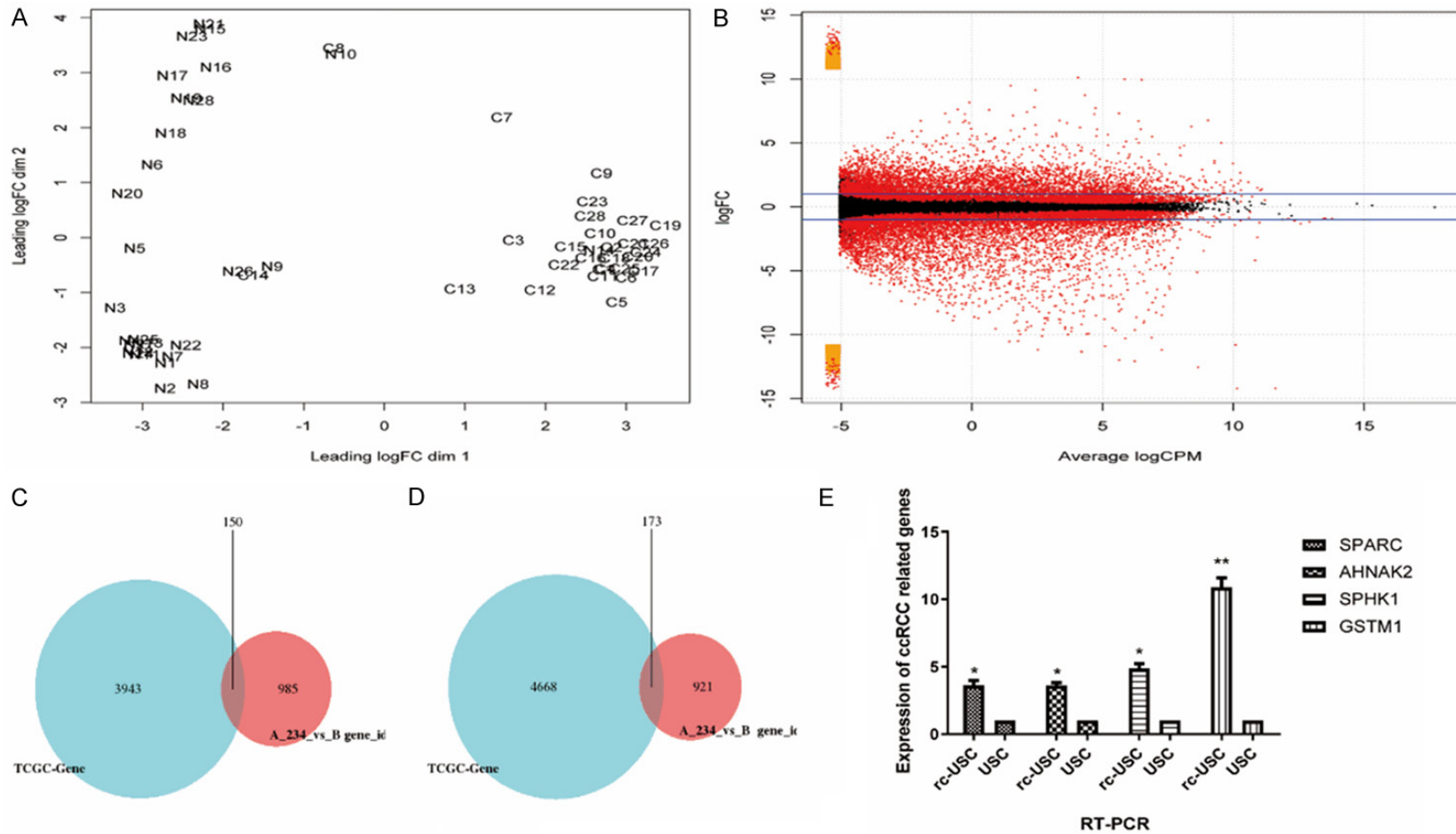
Figure 6. Bioinformatics analysis of DEGs in carcinoma versus paracarcinoma tissues and rc-USC versus USC. A. Quality control showed that the normal (paracarcinoma, N) and cancer (C) samples were separated. B. DEGs of carcinoma and paracarcinoma. C. Venn diagram of DEGs that were upregulated in carcinoma versus paracarcinoma and rc-USC versus USC. D. Venn diagram of DEGs that were downregulated in carcinoma versus paracarcinoma and rc-USC versus USC. E. PCR of ccRCC-associated genes showed these genes overexpressed in rc-USC. $*P<0.05$, $**P<0.01$.

Additionally, rc-USC had increased chromosomal and morphological stability after serial passaging, expressed several proteins associated with ccRCC and presented chromosomal changes similar to those found in cancer tissue based on the FISH assay, but they did not show tumorigenicity. RNA sequencing revealed several differentially expressed lncRNAs and mRNAs, and GO and KEGG enrichment analyses showed small differences in pathways between rc-USC and USC. Bioinformatics analysis of the differentially expressed genes in carcinoma versus paracarcinoma tissues and rc-USC versus USC showed that rc-USC expressed several ccRCC-associated genes, and following PCR verified this result. Furthermore, RCC cells rarely shed into urine until they have penetrated the wall of renal pelvis [29, 30], and all the patients in our study were early stage and without hematuria. These findings suggest that rc-USC are USC that are affected by cancer cells, but not or mixed with cancer cells.

Kidney tumor microenvironment (TME) is consisted of a heterogeneous cell population including tumor cells, extracellular matrix, vessels, stromal cells and various cytokines, and MSC are a common component of the TME since they are a type of stromal cell [31-34]. The most important physiological function of MSC is migrating to injury sites and participating in wound healing, and cancers are considered "wounds that never heal"; therefore, MSC are continuously recruited to tumor sites and become integral components of the TME [13, 35, 36]. The TME enriches tumor-derived exosomes (TEXs) and cytokines via tumoral signaling to both tumor cells and stromal cells and by performing various pathological functions, and MSC are transformed into tumor-associated MSC (TA-MSC) in this microenvironment [13, 32, 37, 38]. Transformed TA-MSC will educate other MSC into TA-MSC via TEXs and play active roles in tumor immunity, tumor growth, tumor angiogenesis, tumor metastasis and therapy resistance [13, 39-41], and TA-MSC also have the differentiation capability of stem cells, such as cancer-associated fibroblasts and endothelial cells [42, 43]. USC can be considered as a type of MSC [10], and our research demonstrated that rc-USC possess some features of cancer and the normal function of USCs; therefore, rc-USC are believed to be TA-MSC.

In our bioinformatics analysis, we found SPARC, AHNAK2, GSTM1 and SPHK1 are overexpressed in ccRCC and promoted tumor development, progression and drug resistance by regulating cell cycle and the Akt/mTOR pathway, supporting epithelial-mesenchymal transition and GSTM1:ASK1 protein-protein interaction [44-47]. These 4 genes were overexpressed in rc-USC compared to normal USC, which suggested these genes were transmitted from cancer cells, made rc-USC present a greater migration and invasion capacity, and potentially involved in the above pathways to promote tumor development. Further studies are suggested to explore the specific functions of rc-USC in tumorigenesis, to identify the rc-USC proportions that may be significantly associated with clinical stages and histological grades of renal tumors, to identify gene-based biomarkers of distinct cell types of RCC, and to monitor tumor recurrence, especially for the patients received partial nephrectomy. rc-USC exhibit substantial phenotypic and functional heterogeneity and might originate from different parts of the nephron in renal tumors. Our RNA sequencing data showed the markers of parietal cells, like CD44, CD24, CD74 and CDH6 [48-50], were high expressed in all samples, and the average FPKM values of these markers were 73.5, 727.8, 7.7 and 43.1, respectively. Therefore, another potential value of rc-USC might be determining the renal tissue origin(s) of USCs.

Voided urine is obtained from both sides of the kidney; therefore, healthy USC and rc-USC mix in the bladder, and rc-USC from tumor side may even mix with healthy USC in renal pelvis. In our study, USC were seeded in 24-well plates, passaged in 6-well plates and finally cultured in 10 cm dishes, therefore, normal USC may be educated into rc-USC during coculturing (**Figure 7**). However, the initial proportion of rc-USC cannot be estimated, and the genetics may change after serial passaging. In addition, recruited stromal cells range in type that might be from outside of kidney, including lymphocytes, Myeloid-derived suppressor cells, macrophages, and bone-marrow mesenchymal stromal cells (BM-MSC) [13, 33, 34, 51]. Therefore, USC from individual wells at P0 should be passaged and researched separately, and single-cell sequencing may better elucidate the cellular composition and transcriptional dynamics
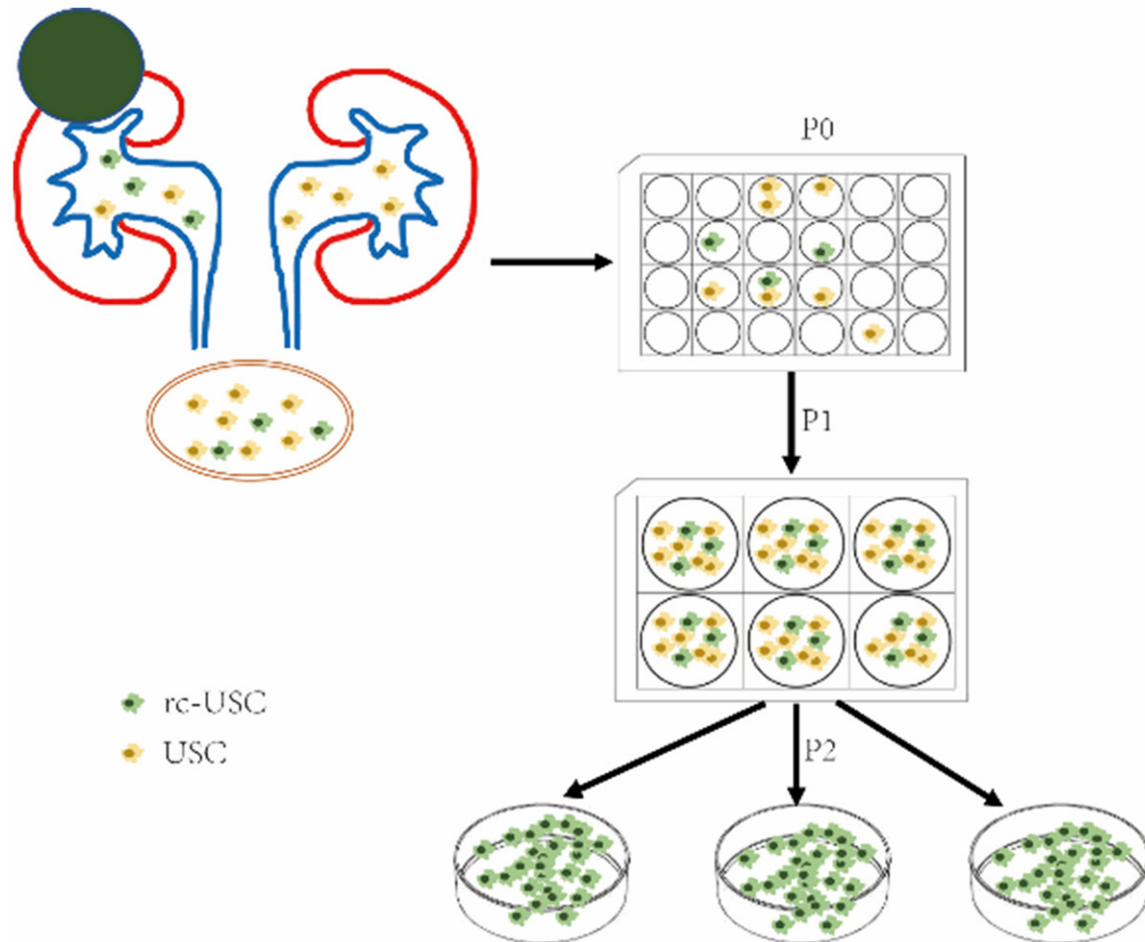
Figure 7. rc-USC may mix and educate USC during collecting, culturing and passaging.

of the diverse cell lineages present in USC from patients with renal cancer. Studies with large sample and other types of RCC are also suggested.

Conclusions

Our results demonstrate that rc-USC from the patients with early stage of ccRCC displayed cancer features at gene and cellular levels, which provides a cell source obtained by noninvasive approach for new diagnosis, predication and disease modeling and therapeutic strategies of ccRCC. As rc-USC are mixed with USC, purification of each cell types is needed for aiding the clinical application of rc-USC.

Acknowledgements

Disclosure of conflict of interest

None.

Address correspondence to: Yunfeng He, Department of Urology, The First Affiliated Hospital of Chongqing Medical University, 1st Youyi Road, Yuzhong District, Chongqing, China. Tel: +86-13206073060; Fax: +86-23-89012919; E-mail: hyf028@126.com

References

[1] Zhang YY, Mcneill E, Tian H, Soker S, Andersson KE, Yoo JJ and Atala A. Urine derived cells are a potential source for urological tissue reconstruction. J Urol 2008; 180: 2226-2233.

[2] Bharadwaj S, Liu GH, Shi YA, Wu RP, Yang B, He TC, Fan YX, Lu XY, Zhou XB, Liu H, Atala A, Rohozinski J and Zhang YY. Multipotential differentiation of human urine-derived stem cells: potential for therapeutic applications in urology. Stem Cells 2013; 31: 1840-1856.

[3] Zhang DY, Wei GH, Li P, Zhou XB and Zhang YY. Urine-derived stem cells: a novel and versatile progenitor source for cell-based therapy and regenerative medicine. Genes Dis 2014; 1: 8-17.

[4] Pavathuparambil Abdul Manaph N, Al-Hawwas M, Bobrovskaya L, Coates PT and Zhou XF. Urine-derived cells for human cell therapy. Stem Cell Res Ther 2018; 9: 189.

[5] Chun SY, Kim HT, Lee JS, Kim MJ, Kim BS, Kim BW and Kwon TG. Characterization of urine-derived cells from upper urinary tract in Patients with bladder cancer. Urology 2012; 79: 1186, e1-e7.

[6] Liu GH, Wu RP, Yang B, Deng CH, Lu XB, Walker SJ, Ma PX, Mou S, Atala A and Zhang YY. Human urine-derived stem cell differentiation to endothelial cells with barrier function and nitric oxide production. Stem Cells Transl Med 2018; 7: 686-698.

[7] Yang QY, Chen X, Zheng T, Han DY, Zhang H, Shi YN, Bian J, Sun XZ, Xia K, Liang XY, Liu GH, Zhang YY and Deng CH. Transplantation of human urine-derived stem cells transfected with pigment epithelium-derived factor to protect erectile function in a rat model of cavernous nerve injury. Cell Transplant 2016; 25: 1987-2001.

[8] Liu GH, Wang XS, Sun XZ, Deng CH, Atala A and Zhang YY. The effect of urine-derived stem cells expressing VEGF loaded in collagen hydrogels on myogenesis and innervation following after subcutaneous implantation in nude mice. Biomaterials 2013; 34: 8617-29.

[9] Dong XY, Zhang T, Liu Q, Zhu JZ, Zhao J, Li J, Sun BS, Ding GL, Hu XY, Yang ZX, Zhang YY and Li LK. Beneficial effects of urine-derived stem cells on fibrosis and apoptosis of myocardial, glomerular and bladder cells. Mol Cell Endocrinol 2016; 427: 21-32.

[10] Ji XL, Wang M, Chen F and Zhou JM. Urine-derived stem cells: the present and the future. Stem Cells Int 2017; 2017: 4378947.

[11] Bharadwaj S, Liu GH, Shi YA, Markert C, Andersson KE, Atala A and Zhang YY. Characterization of urine-derived stem cells obtained from upper urinary tract for use in cell-based urological tissue engineering. Tissue Eng Part A 2011; 17: 2123-32.

[12] Hsieh JJ, Purdue MP, Signoretti S, Swanton C, Albiges L, Schmidinger M, Heng DY, Larkin J and Ficarra V. Renal cell carcinoma. Nat Rev Dis Primers 2017; 3: 17009.

[13] Shi YF, Du LM, Lin LY and Wang Y. Tumour-associated mesenchymal stem/stromal cells: emerging therapeutic targets. Nat Rev Drug Discov 2017; 16: 35-52.

[14] Dagher J, Dugay F, Verhoest G, Cabillic F, Jaillard S, Henry C, Arlot-Bonnemains Y, Bensalah K, Oger E, Vigneau C, Rioux-Leclercq N and Belaud-Rotureau MA. Histologic prognostic factors associated with chromosomal imbalances in a contemporary series of 89 clear cell renal cell carcinomas. Hum Pathol 2013; 44: 2106-15.

[15] Sanfrancesco JM, Eble JN, Grignon DJ, Wang MS, Zhang SB, Sundaram CP, Idrees MT, Pili R, Kouba E and Cheng L. Preservation of truncal genomic alterations in clear cell and papillary renal cell carcinomas with sarcomatoid features: an intra- and intertumoral, multifocal fluorescence in situ hybridization analysis reveals limited genetic heterogeneity. Mol Carcinog 2017; 56: 2527-2537.

[16] Gronwald J, Störkel S, Holtgreve-Grez H, Hadaczek P, Brinkschmidt C, Jauch A, Lubinski J and Cremer T. Comparison of DNA gains and losses in primary renal clear cell carcinomas and metastatic sites: importance of 1q and 3p copy number changes in metastatic events. Cancer Res 1997; 57: 481-7.

[17] Sangoi AR, Karamchandani J, Kim J, Pai RK and McKenney JK. The use of immunohistochemistry in the diagnosis of metastatic clear cell renal cell carcinoma: a review of PAX-8, PAX-2, hKIM-1, RCCma, and CD10. Adv Anat Pathol 2010; 17: 377-93.

[18] Douville J, Beaulieu R and Balicki D. ALDH1 as a functional marker of cancer stem and progenitor cells. Stem Cells Dev 2009; 18: 17-25.

[19] Mjønes PG, Nordrum IS, Qvigstad G, Sørdal Ø, Rian LL and Waldum HL. Expression of erythropoietin and neuroendocrine markers in clear cell renal cell carcinoma. APMIS 2017; 125: 213-222.

[20] Song DJ, Yue LF, Wu G, Ma SS, Guo LH, Yang HY, Liu QL, Zhang D, Xia ZG, Wang L, Zhang JJ, Zhao W, Guo F and Wang JX. Assessment of promoter methylation and expression of SIX2 as a diagnostic and prognostic biomarker in Wilms' tumor. Tumour Biol 2015; 36: 7591-8.

[21] Chen ZX, Luo SJ, Chen YL, Xie XM, Du ZB and Jiang L. High expression of NPRL2 is linked to poor prognosis in patients with prostate cancer. Hum Pathol 2018; 76: 141-148.

[22] Xu L, Pelosof L, Wang R, McFarland HI, Wu WW, Phue JN, Lee CT, Shen RF, Juhl H, Wu LH, Alterovitz WL, Petricon E and Rosenberg AS. NGS evaluation of colorectal cancer reveals interferon gamma dependent expression of immune checkpoint genes and identification of novel IFNγ induced genes. Front Immunol 2020; 11: 224.

[23] Zygmunt M, Hoinkis D, Hajto J, Piechota M, Skupień-Rabian B, Jankowska U, Kędracka-Krok S, Parkitna JR and Korostyński M. Expression of alternatively spliced variants of the Dclk1 gene is regulated by psychotropic drugs. BMC Neurosci 2018; 19: 55.

[24] Wang LL, Chen YH, Guan CY, Zhao ZJ, Li Q, Yang JG, Mo J, Wang B, Wu W, Yang XH, Song LB and Li J. Using low-risk factors to generate non-integrated human induced pluripotent stem cells from urine-derived cells. Stem Cell Res Ther 2017; 8: 245.

[25] Wu SF, Wang Z, Bharadwaj S, Hodges SJ, Atala A and Zhang YY. Implantation of autologous urine derived stem cells expressing vascular endothelial growth factor for potential use in genitourinary reconstruction. J Urol 2011; 186: 640-7.

[26] Wu RP, Liu GH, Yang B, Fan YX, Rohozinski J, Atala A and Zhang YY. Human urine-derived stem cells originate from parietal stem cells. J Urol 2014; 191: e217.

[27] Pippin JW, Sparks MA, Glenn ST, Buitrago S, Coffman TM, Duffield JS, Gross KW and Shankland SJ. Cells of renin lineage are progenitors of podocytes and parietal epithelial cells in experimental glomerular disease. Am J Pathol 2013; 183: 542-57.

[28] Dominici M, Le BK, Mueller I, Slaper-Cortenbach I, Marini F, Krause D, Deans R, Keating A, Prockop D and Horwitz E. Minimal criteria for defining multipotent mesenchymal stromal cells. The international society for cellular therapy position statement. Cytotherapy 2006; 8: 315-7.

[29] Dubal SB, Pathuthara S, Ajit D, Menon S and Kane SV. Case report of renal cell carcinoma diagnosed in voided urine confirmed by CD10 immunocytochemistry. Acta Cytol 2011; 55: 372-6.

[30] Sullivan PS, Chan JB, Levin MR and Kane SV. Urine cytology and adjunct markers for detection and surveillance of bladder cancer. Am J Transl Res 2010; 2: 412-40.

[31] Hui LL and Chen Y. Tumor microenvironment: sanctuary of the devil. Cancer Lett 2015; 368: 7-13.

[32] Meng WR, Hao YY, He CS, Li L and Zhu GQ. Exosome-orchestrated hypoxic tumor microenvironment. Mol Cancer 2019; 18: 57.

[33] Vuong L, Kotecha RR, Voss MH and Hakimi AA. Tumor microenvironment dynamics in clear-cell renal cell carcinoma. Cancer Discov 2019; 9: 1349-1357.

[34] Mier JW. The tumor microenvironment in renal cell cancer. Curr Opin Oncol 2019; 31: 194-199.

[35] Schildberg FA and Donnenberg VS. Stromal cells in health and disease. Cytometry A 2018; 93: 871-875.

[36] Caplan AI and Correa D. The MSC: an injury drugstore. Cell Stem Cell 2011; 9: 11-5.

[37] Ren GW, Zhao X, Wang Y, Zhang X, Chen XD, Xu CL, Yuan ZR, Roberts AI, Zhang LY, Zheng B, Wen T, Han YY, Rabson AB, Tischfield JA, Shao CS and Shi YF. CCR2-dependent recruitment of macrophages by tumor-educated mesenchymal stromal cells promotes tumor development and is mimicked by TNFα. Cell Stem Cell 2012; 11: 812-24.

[38] Whiteside TL. Exosome and mesenchymal stem cell cross-talk in the tumor microenvironment. Semin Immunol 2018; 35: 69-79.

[39] Klemm F and Joyce JA. Microenvironmental regulation of therapeutic response in cancer. Trends Cell Biol 2015; 25: 198-213.

[40] De BA, Pauwels P, Hensen K, Rummens JL, Westbroek W, Hendrix A, Maynard D, Denys H, Lambein K, Braems G, Gespach C, Bracke M and Wever OD. Bone marrow-derived mesenchymal stem cells promote colorectal cancer progression through paracrine neuregulin 1/HER3 signalling. Gut 2013; 62: 550-60.

[41] Koh BI and Kang YB. The pro-metastatic role of bone marrow-derived cells: a focus on MSCs and regulatory T cells. EMBO Rep 2012; 13: 412-22.

[42] Quante M, Tu SP, Tomita H, Gonda T, Wang SS, Takashi S, Baik GH, Shibata W, Diprete B, Betz KS, Friedman R, Varro A, Tycko B and Wang TC. Bone marrow-derived myofibroblasts contribute to the mesenchymal stem cell niche and promote tumor growth. Cancer Cell 2011; 19: 257-72.

[43] Sun BC, Zhang SW, Ni CS, Zhang DF, Liu YX, Zhang WZ, Zhao XL, Zhao CH and Shi MX. Correlation between melanoma angiogenesis and the mesenchymal stem cells and endothelial progenitor cells derived from bone marrow. Stem Cells Dev 2005; 14: 292-8.

[44] Gagliano N, Pettinari L, Aureli M, Martinelli C, Colombo E, Costa F, Carminati R, Volpari T, Colombo G, Milzani A, Dalle-Donne I and Gioia M. Malignant phenotype of renal cell carcinoma cells is switched by ukrain administration in vitro. Anticancer Drugs 2011; 22: 749-62.

[45] Wang ML, Li XF, Zhang J, Yang Q, Chen WQ, Jin WL, Huang YR, Yang R and Gao WQ. AHNAK2 is a novel prognostic marker and oncogenic protein for clear cell renal cell carcinoma. Theranostics 2017; 7: 1100-1113.

[46] Coric VM, Simic TP, Pekmezovic TD, Basta-Jo-vanovic GM, Savic-Radojevic AR, Radojevic-Sk-odric SM, Matic MG, Suvakov SR, Dragicevic DP, Radic TM, Dzamic ZM and Pljesa-Ercegov-ac MS. GSTM1 genotype is an independent prognostic factor in clear cell renal cell carci-noma. Urol Oncol 2017; 35: 409-417.

[47] Xu Y, Dong B, Wang J, Zhang J, Xue W and Huang Y. Sphingosine kinase 1 overexpression contributes to sunitinib resistance in clear cell renal cell carcinoma. Oncoimmunology 2018; 7: e1502130.

[48] Fatima H, Moeller MJ, Smeets B, Yang HC, D'Agati VD, Alpers CE and Fogo AB. Parietal epithelial cell activation marker in early recur-rence of FSGS in the transplant. Clin J Am Soc Nephrol 2012; 7: 1852-8.

[49] Kuppe C, Leuchtle K, Wagner A, Kabgani N, Saritas T, Puelles VG, Smeets B, Hakroush S, van der Vlag J, Boor P, Schiffer M, Gröne HJ, Fogo A, Floege J and Moeller MJ. Novel parietal epithelial cell subpopulations contribute to fo-cal segmental glomerulosclerosis and glomer-ular tip lesions. Kidney Int 2019; 96: 80-93.

[50] Lindgren D, Boström AK, Nilsson K, Hansson J, Sjölund J, Möller C, Jirström K, Nilsson E, Land-berg G, Axelson H and Johansson ME. Isolation and characterization of progenitor-like cells from human renal proximal tubules. Am J Pathol 2011; 178: 828-37.

[51] Hsiao WC, Sung SY, Liao CH, Wu HC and Hsieh CL. Vitamin D3-inducible mesenchymal stem cell-based delivery of conditionally replicating adenoviruses effectively targets renal cell car-cinoma and inhibits tumor growth. Mol Pharm 2012; 9: 1396-408.

Table S1. The sequences of RT-qPCR primers

Primer	Sequence
Human GAPDH	Fwd: CAGCGACACCCACTCCTC
	Rev: CGGACACATTGGGGGTAG
Human PAX2	Fwd: ATCAACAGAATCATCCGGACCAA
	Rev: GGAACAATGGTGTGGCCAGG
Human SIX2	Fwd: AGGCCAAGGAAAGGGAGAAC
	Rev: GAGCTGCCTAACACCGACTT
Human NCAM1	Fwd: CCGCCTTCTCGAAAGATGAGT
	Rev: CTTCTACGGGGCCCTTCTCG
Human ALDH1	Fwd: CAACAGAGGTTGGCAAGTTGA
	Rev: CCAAGTCGGCATCAGCTAAC
Human TUBBP1	Fwd: TCTCAGCTTCAAGGGAGGTG
	Rev: AGCTGAGTGAGGGAGGTAGA
Human HS3ST3A1	Fwd: CAACAAGACCAAGGGCTTCC
	Rev: AGGTTGAAAGGCCGGTAGAA
Human AC117402.1	Fwd: TTGAACCAGCATTGCATCCC
	Rev: CGAATCCAGCAGCACATCAA
Human GSTM1	Fwd: GCTTTGAGGGCTTGGAGAAG
	Rev: GAACACAGGTCTTGGGAGGA
Human AC138028.1	Fwd: CTGCTTCTCCTTCCTCAGGT
	Rev: CACAGGCAAAGGAAACCACA
Human HP	Fwd: GGCATTATGAAGGCAGCACA
	Rev: AGATCCCAGTCGCATACCAG
Human NEAT1	Fwd: TTACCAGCTTCCTCCTGGTG
	Rev: AGTCTGACGCCCATCTTTCA
Human IL1RL1	Fwd: ATGGAACACACGGGAAGTCT
	Rev: GCAAACTGAGGGCCAAGAAA
Human AP000866.6	Fwd: AGCCCTAAACCAAAGGCACT
	Rev: CCAGTTGATGCCAATAATGCTG
Human AC009318.1	Fwd: TTGGAAAGCTGCTCACCATC
	Rev: TGCCTGTGTAATGGCAAGTC
Human SPARC	Fwd: TGCGGGTGAAGAAGATCCAT
	Rev: CTGCCAGTGTACAGGGAAGA
Human AHNAK2	Fwd: ATCCTGGTGGAAGCGAGATT
	Rev: CTTCAGCGTCACCTCTGTTG
Human SPHK1	Fwd: TTGGTATATGTGCCCGTGGT
	Rev: CTGCAAACACACCTTTCCCA

Methods of RNA sequencing

Sample collection and preparation

RNA quantification and qualification

RNA degradation and contamination was monitored on 1% agarose gels.

RNA purity was checked using the NanoPhotometer® spectrophotometer (IMPLEN, CA, USA).

RNA concentration was measured using Qubit® RNA Assay Kit in Qubit® 2.0 Flurometer (Life Technologies, CA, USA).

RNA integrity was assessed using the RNA Nano 6000 Assay Kit of the Bioanalyzer 2100 system (Agilent Technologies, CA, USA).

Library preparation for Transcriptome sequencing

A total amount of 3 μg RNA per sample was used as input material for the RNA sample preparations. Sequencing libraries were generated using NEBNext® UltraTM RNA Library Prep Kit for Illumina® (NEB, USA) following manufacturer's recommendations and index codes were added to attribute sequences to each sample. Briefly, mRNA was purified from total RNA using poly-T oligo-attached magnetic beads. Fragmentation was carried out using divalent cations under elevated temperature in NEBNext First Strand Synthesis Reaction Buffer (5×). First strand cDNA was synthesized using random hexamer primer and M-MuLV Reverse Transcriptase (RNase H-). Second strand cDNA synthesis was subsequently performed using DNA Polymerase I and RNase H. Remaining overhangs were converted into blunt ends via exonuclease/polymerase activities. After adenylation of 3' ends of DNA fragments, NEBNext Adaptor with hairpin loop structure were ligated to prepare for hybridization. In order to select cDNA fragments of preferentially 150~200 bp in length, the library fragments were purified with AMPure XP system (Beckman Coulter, Beverly, USA). Then 3 μl USER Enzyme (NEB, USA) was used with size-selected, adaptor-ligated cDNA at 37°C for 15 min followed by 5 min at 95°C before PCR. Then PCR was performed with Phusion High-Fidelity DNA polymerase, Universal PCR primers and Index (X) Primer. At last, PCR products were purified (AMPure XP system) and library quality was assessed on the Agilent Bioanalyzer 2100 system.

Clustering and sequencing (genechem experimental department)

The clustering of the index-coded samples was performed on a cBot Cluster Generation System using TruSeq PE Cluster Kit v3-cBot-HS (Illumia) according to the manufacturer's instructions. After cluster generation, the library preparations were sequenced on an Illumina Hiseq platform and 125 bp/150 bp paired-end reads were generated.

Data analysis

Quality control

Raw data (raw reads) of fastq format were firstly processed through in-house perlscripts. In this step, clean data (clean reads) were obtained by removing reads containing adapter, reads containing ploy-N and low quality reads from raw data. At the same time, Q20, Q30 and GC content the clean data were calculated. All the downstream analyses were based on the clean data with high quality.

Reads mapping to the reference genome

Reference genome and gene model annotation files were downloaded from genome website directly. Index of the reference genome was built using STAR and paired-end clean reads were aligned to the

reference genome using STAR (v2.5.1b). STAR used the method of Maximal Mappable Prefix (MMP) which can generate a precise mapping result for junction reads.

Quantification of gene expression level

HTSeq v0.6.0 was used to count the reads numbers mapped to each gene. And then FPKM of each gene was calculated based on the length of the gene and reads count mapped to this gene. FPKM, expected number of Fragments Per Kilobase of transcript sequence per Millions base pairs sequenced, considers the effect of sequencing depth and gene length for the reads count at the same time, and is currently the most commonly used method for estimating gene expression levels.

Differential expression analysis

(For DESeq2 with biological replicates) Differential expression analysis of two conditions/groups (two biological replicates per condition) was performed using the DESeq2 R package (1.10.1). DESeq2 provide statistical routines for determining differential expression in digital gene expression data using a model based on the negative binomial distribution. The resulting *P*-values were adjusted using the Benjamini and Hochberg's approach for controlling the false discovery rate. Genes with an adjusted *P*-value <0.05 found by DESeq2 were assigned as differentially expressed.

(For edgeR without biological replicates) Prior to differential gene expression analysis, for each sequenced library, the read counts were adjusted by edgeR program package through one scaling normalized factor. Differential expression analysis of two conditions was performed using the edgeR R package (3.12.1). The *P* values were adjusted using the Benjamini & Hochberg method. Corrected *P*-value of 0.05 and absolute foldchange of 2 were set as the threshold for significantly differential expression.

GO and KEGG enrichment analysis of differentially expressed genes

Gene Ontology (GO) enrichment analysis of differentially expressed genes was implemented by the cluster Profiler R package, in which gene length bias was corrected. GO terms with corrected *P* value less than 0.05 were considered significantly enriched by differential expressed genes.

KEGG is a database resource for understanding high-level functions and utilities of the biological system, such as the cell, the organism and the ecosystem, from molecular-level information, especially large-scale molecular datasets generated by genome sequencing and other high-through put experimental technologies (http://www.genome.jp/kegg/). We used cluster Profiler R package to test the statistical enrichment of differential expression genes in KEGG pathways.

SNP analysis

GATK2 (v3.2.1) software was used to perform SNP calling and SnpEff software was used to annotation for the Variablesite.

AS analysis

Alternative Splicing is an important mechanism for regulate the expression of genes and the variable of protein. rMATS (3.2.1) software was used to analysis the ASevent.

Fusion analysis

Fusion gene is referring to the two genes of all or part of the sequences perform fusion, results of the chimeric gene, usually caused by reasons such as chromosome translocation and problem. We used SOAPfuse (1.27) software analysis and detection of fusion genes.

Table S2. The number of formations of rc-USC and USC mono-clone

| Group	Serial number	Male/female	Age	Time of first clone appearance (day)	Volume (ml)	No. of clones	Mean ± SD
rc-USC	1	M	61	3	180	22	18.7±2.7*
	2	F	52	4	140	20	
	3	M	56	4	120	15	
	4	M	47	3.5	160	16	
	5	M	45	4	150	19	
	6	F	66	5	200	20	
USC	1	F	48	6	200	12	11.2±2.1
	2	M	59	7	190	11	
	3	M	38	5	200	15	
	4	F	45	7	200	10	
	5	M	55	8	200	10	
	6	M	57	7	200	9	

*$P<0.05$, compared to USC.

Table S3. Basic characters of patients for sequencing

| No.	Gender	Age	T stage	Operation	Pathology result	Number of cells
1 (excluded)	Male	49	T1bN0M0	Radical	XP11.2 RCC	$5.2×10^6$
2	Male	59	T1bN0M0	Partial	ccRCC, G2	$3.2×10^6$
3	Female	57	T1bN0M0	Radical	ccRCC, G2	$3.1×10^6$
4	Female	56	T1bN0M0	Radical	ccRCC, G2	$6.7×10^5$
5	Male	52	-		-	$1.2×10^6$
6	Female	49	-		-	$2.0×10^6$
7	Male	52	-		-	$2.9×10^6$
8	Female	44	-		-	$8.4×10^5$

4

Patient No.1
Male, 49y
XP11.2 RCC
T1bN0M0
(excluded)
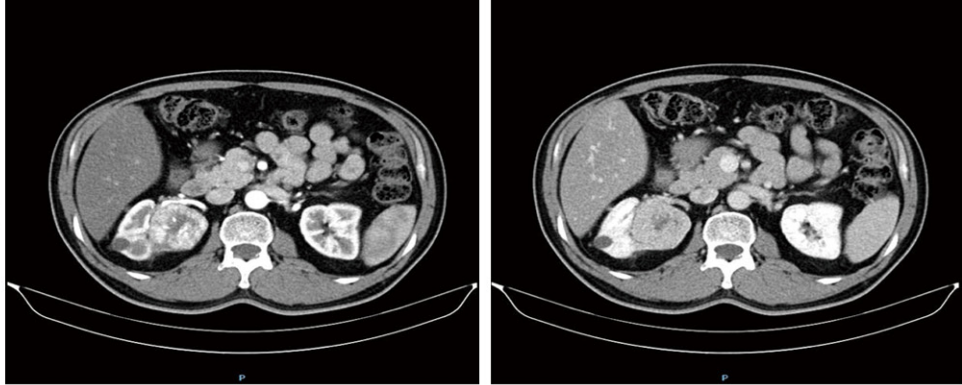
Patient No.2
Male, 59y
ccRCC, G2
T1bN0M0
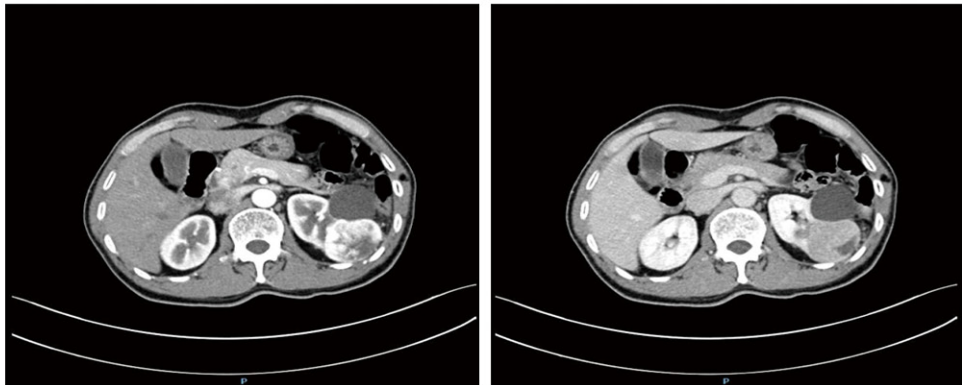
Patient No.3
Female, 57y
ccRCC, G2
T1bN0M0
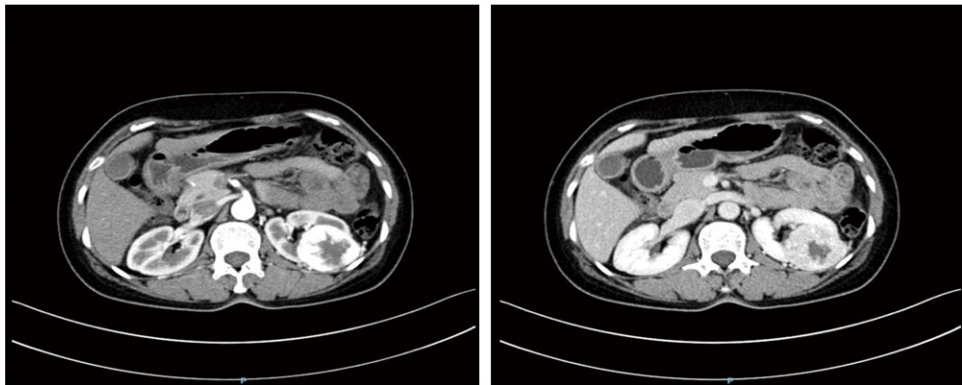
Patient No.4
Female, 56y
ccRcc, G2
T2N0M0

Figure S1. CT images of the sequencing patients.

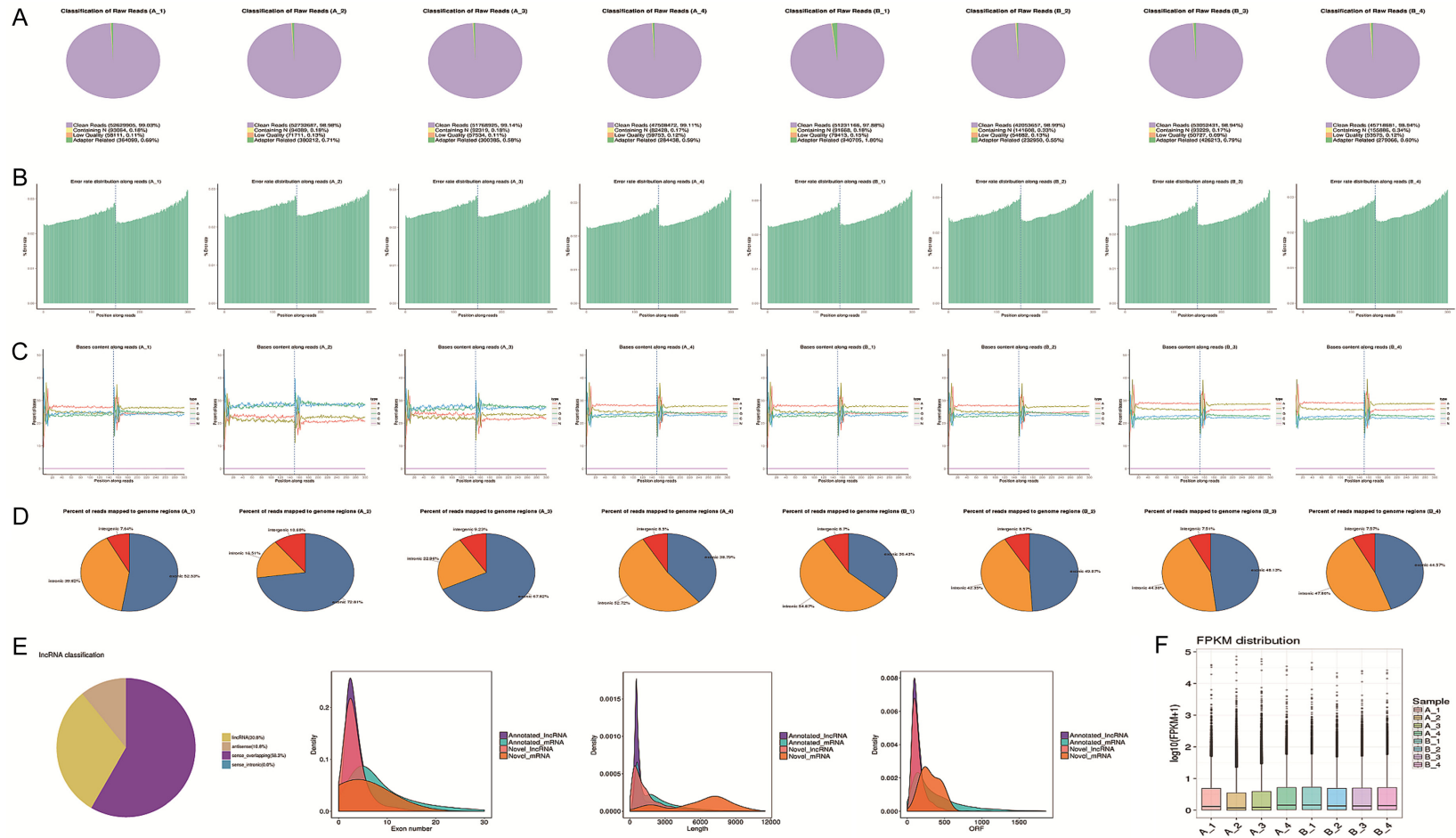**Figure S2.** Quality control of RNA sequencing.

6

Table S4. Top 5 upregulated and 5 downregulated mRNAs in rc-USCs and USCs

Gene symbol	Gene ID	Location	A FPKM	B FPKM	Log$_2$FC	P value	P adjust	Trend
CA7	ENSG00000168748	chr16:66840546-66891710	2.258136	0.015162	6.962732	4.05E-07	0.0008	Up
SST	ENSG00000157005	chr3:187668906-187670399	195.9206	11.10857	4.49789	2.34E-06	0.002252	Up
TM4SF19	ENSG00000145107	chr3:196319342-196338503	3.71713	0.294766	4.013802	3.02E-05	0.014516	Up
GLIS1	ENSG00000174332	chr1:53506237-53739900	2.117878	0.219721	3.612001	1.69E-05	0.009196	Up
HS3ST3A1	ENSG00000153976	chr17:13495689-13602787	7.031899	0.834607	3.386565	1.12E-06	0.001683	Up
SEC22B	ENSG00000265808	chr1:120150898-120342591	4.509805	13.47802	-2.03183	2.10E-06	0.002207	Down
SCEL	ENSG00000136155	chr13:77535674-77645263	4.174183	28.02549	-2.52995	8.84E-06	0.006905	Down
MOB4	ENSG00000115540	chr2:197515571-197553699	1.620038	9.256928	-2.67592	2.92E-06	0.00267	Down
ANP32E	ENSG00000143401	chr1:150218417-150236156	1.358215	12.42732	-2.88619	1.67E-05	0.009196	Down
RHOQ	ENSG00000119729	chr2:46541806-46583121	3.227748	21.17007	-2.95399	7.41E-05	0.027259	Down

Table S5. Top 5 upregulated and 5 downregulated LncRNAs in rc-USCs for PCR verification

Gene symbol	Gene ID	Location	A FPKM	B FPKM	Log$_2$FC	P value	P adjust	Trend
TUBBP1	ENSG00000127589	chr8:30351873-30353518	9.201369	0.167297	6.029688	1.87E-06	0.00213	Up
HS3ST3A1	ENSG00000153976	chr17:13495689-13602787	7.031899	0.834607	3.386565	1.12E-06	0.001683	Up
AC117402.1	ENSG00000206532	chr3:110886941-110969962	7.46911	0.42881	4.77108	7.37E-05	0.027259	Up
GSTM1	ENSG00000134184	chr1:109687814-109709039	5.297829	0.217101	4.908912	2.00E-07	0.000549	Up
AC138028.1	ENSG00000182376	chr16:88718615-88785211	1.765749	0.072957	5.265973	2.12E-06	0.002207	Up
HP	ENSG00002257017	chr16:72054592-72061055	0	2.715248	-10.5146	0.000111	0.036837	Down
NEAT1	ENSG00000245532	chr11:65422774-65445540	0.03711	14.13095	-8.5493	3.57E-05	0.016749	Down
IL1RL1	ENSG00000115602	chr2:102311502-102352037	0.036298	2.36716	-5.65453	0.000161	0.046721	Down
AP000866.6	ENSG00000279342	chr11:124789240-124792818	0.77873	2.536066	-3.57627	0.000168	0.048178	Down
AC009318.1	ENSG00000257176	chr12:29279613-29329536	0.259315	1.511793	-3.35865	1.73E-05	0.009278	Down

Table S6. GO enrich significant pathways and genes

Category	ID	Description	GeneRatio	BgRatio	*P*value	Padj	geneID	Count
CC	GO:0005578	proteinaceous extracellular matrix	8/70	313/15404	8.40E-05	0.009279	COL6A3/SPARC/AMTN/ZP4/ADAMTSL1/CRISPLD2/TIMP2/IL1RL1	8
CC	GO:0042383	sarcolemma	5/70	105/15404	0.000114	0.009279	KCND3/COL6A3/DYSF/AHNAK2/FLNC	5
CC	GO:0031012	extracellular matrix	8/70	369/15404	0.00026	0.014114	COL6A3/SPARC/AMTN/ZP4/ADAMTSL1/CRISPLD2/TIMP2/IL1RL1	8